



**HAL**  
open science

## Double Trouble Mutations Underlie Mitochondrial Dynamics Disorders in a Severe Form of Charcot-Marie-Tooth Disease

Angela Puma, Samuel Guilbault, Emmanuelle C Genin, Christophe Duranton, Isabelle Rubera, Nathalie Bonello-Palot, Véronique Paquis-Flucklinger, Sabrina Sacconi, Saïd Bendahhou

► **To cite this version:**

Angela Puma, Samuel Guilbault, Emmanuelle C Genin, Christophe Duranton, Isabelle Rubera, et al.. Double Trouble Mutations Underlie Mitochondrial Dynamics Disorders in a Severe Form of Charcot-Marie-Tooth Disease. *Journal of Biotechnology and Biomedicine*, 2023, 06 (04), pp.468-475. 10.26502/jbb.2642-91280109 . hal-04275405

**HAL Id: hal-04275405**

**<https://hal.science/hal-04275405v1>**

Submitted on 8 Nov 2023

**HAL** is a multi-disciplinary open access archive for the deposit and dissemination of scientific research documents, whether they are published or not. The documents may come from teaching and research institutions in France or abroad, or from public or private research centers.

L'archive ouverte pluridisciplinaire **HAL**, est destinée au dépôt et à la diffusion de documents scientifiques de niveau recherche, publiés ou non, émanant des établissements d'enseignement et de recherche français ou étrangers, des laboratoires publics ou privés.

Public Domain


**Research Article**

## Double Trouble Mutations Underlie Mitochondrial Dynamics Disorders in a Severe Form of Charcot-Marie-Tooth Disease

Angela Puma<sup>1,2</sup>, Samuel Guilbault<sup>2</sup>, Emmanuelle C Genin<sup>3</sup>, Christophe Duranton<sup>2</sup>, Isabelle Rubera<sup>2</sup>, Nathalie Bonello-Palot<sup>4</sup>, Véronique Paquis-Flucklinger<sup>3</sup>, Sabrina Sacconi<sup>1</sup>, Saïd Bendahhou<sup>2\*</sup>

### Abstract

Charcot-Marie-Tooth disease type 2A (CMT2A) is an inherited axonal peripheral neuropathy mainly caused by mutations in the mitofusin 2 (*MFN2*) gene encoding for the MFN2 protein, a GTPase involved in the mitochondrial dynamics and bioenergetics. We identified a novel mutation, that was inherited from her mother, in the MFN2 protein (Met234Ile) in a Charcot-Marie-Tooth patient. She has also a variant of uncertain significance (Thr36Ala), in the *PMP22* gene, encoding for peripheral myelin protein 22, inherited from her father. The patient presented severe sensorimotor neuropathy with early onset. The mother presented a distal muscle atrophy in the legs, the father was asymptomatic. To show the pathogenicity of these mutations, we characterized the structure, adenosine triphosphate (ATP) content, bioelectric characteristics and functions of mitochondria in cultured primary fibroblasts obtained from the proband and her parents. Under normal culture conditions, mitochondria showed normal morphology. Under oxidative stress conditions, ATP production was reduced and the proband cells showed a decrease of the mitochondrial fusion with small connected networks and a decrease of the mitochondrial volume. The alteration of the mitochondrial network only when cells are challenged in aerobiosis testifies to the fragility of mitochondria, which are unable to meet the metabolic needs of neurons. Interestingly, fibroblasts derived from the two parents did not show any change.

These results support the hypothesis that the mutation in the *MFN2* gene altering mitochondrial bioenergetics and fusion causes axonal sensory-motor neuropathy. We speculate that *PMP22* may promote mitochondrial dysfunction, myelin having a role in mitochondrial metabolism.

**Keywords:** MFN2; CMT2A; PMP22; Fibroblasts; Mitochondrial network; Fusion.

### Introduction

Charcot-Marie-Tooth disease (CMT) also known as hereditary sensory-motor neuropathies (HMSN) is the most common inherited neuropathy, with a prevalence of 1:2500 [1]. Depending on the motor conduction velocity (MCV) found on the median nerve at electrodiagnostic evaluation (EDX), CMTs can be classified into three principal groups, demyelinating (MCV  $\leq 35$  m/sec), intermediaries (MCV between 35 and 45 m/sec) or axonal ( $\geq 45$  m/sec)[2]. As far as demyelinating forms are concerned, CMT1A is the most frequent form. It is due to a 1.4 Mb duplication on chromosome 17p11.2 that includes the *PMP22* gene encoding for the peripheral myelin protein 22 [3]. More rarely ( $<5\%$  of cases) is caused by a point mutation in the same

### Affiliation:

<sup>1</sup>Université Côte d'Azur, Centre Hospitalier Universitaire de Nice, Système Nerveux Périphérique & Muscle, Hôpital Pasteur 2, 30 voie Romaine CS, Nice, France

<sup>2</sup>Université Côte d'Azur, CNRS, LP2M, Labex ICST, Faculté de Médecine, Nice, France

<sup>3</sup>Université Côte d'Azur, Inserm U1081, CNRS UMR7284, IRCAN, CHU de Nice, Nice, France

<sup>4</sup>APHM, CHU Timone, Département de Génétique Médicale, Marseille, France, INSERM, MMG, U 1251, Marseille, France, Aix Marseille Univ, Marseille, France

### \*Corresponding author:

Saïd Bendahhou, Université Côte d'Azur, CNRS, LP2M, Labex ICST, Faculté de Médecine, Nice, France.

**Citation:** Angela Puma, Samuel Guilbault, Emmanuelle C Genin, Christophe Duranton, Isabelle Rubera, Nathalie Bonello-Palot, Véronique Paquis-Flucklinger, Sabrina Sacconi, Saïd Bendahhou. Double Trouble Mutations Underlie Mitochondrial Dynamics Disorders in a Severe Form of Charcot-Marie-Tooth Disease. *Journal of Biotechnology and Biomedicine*. 6 (2023): 468-475.

**Received:** July 17, 2023

**Accepted:** July 24, 2023

**Published:** October 11, 2023

gene [4]. CMT1A has a classic CMT phenotype, *i.e.* length-dependent. The clinical severity is highly variable. The onset age is in the first decade in 75% of cases. Clinically, patients present with distal weakness/atrophy, sensory loss and cavus feet. Deep reflexes are abolished. [5].

PMP22 is a 22-kD protein that makes up 2-5% of myelin in the peripheral nervous system. Its function is unclear. It probably plays a role in Schwann cell growth and differentiation. It has been hypothesized that a point mutation of PMP22 makes the protein dysfunctional while duplication may compromise stoichiometry and interactions with other myelin proteins [6].

Axonal CMTs, known as CMT2A, are mostly associated with mutations in the Mitofusin 2 (*MFN2*) gene. *MFN2* gene, located on chromosome 1p36.22, is encoding for MFN2 protein. [7]. CMT2A has an autosomal dominant transmission in 90% of cases. [8]. The age of onset varies within the same family and ranges from one year to the sixth decade, although most individuals develop manifestations in the first and second decades of life [9]. Its clinical phenotype is more complex than that of CMT1A, as it may involve the optic nerve [10] and the pyramidal tract [11]. Distal weakness and atrophy predominate over sensory signs. Deep tendon reflexes are usually absent, but can be present. Lesions of the cerebral white matter have been described [10,12,13]. Additional signs are postural tremor [14] and vocal cord paralysis with hoarse voice [15]. Some individuals with pathogenic variants of *MFN2* are asymptomatic [16]; however, the disease may manifest later in life [17].

*MFN2* is an ubiquitous protein of 757 amino acids belonging to the mitochondrial transmembrane GTPases family. It contains a GTPase domain, two transmembrane domains and two coiled-coil regions that mediate binding to other mitofusin molecules [18]. This protein is crucial for mitochondrial dynamics and is involved mainly in the processes of mitochondrial fusion and displacement of mitochondria within the cell [19], [20].

Although *MFN2* is ubiquitously expressed, mutations in this gene cause mainly neuronal dysfunction. Cases of double trouble have been described in the literature to indicate the presence of two different mutations in genes involved in CMT that can interact to give new, sometimes more pronounced phenotypes [21,22,23]. Here, we report two genetic mutations in the heterozygous state in a patient, one inherited from the mother on the *MFN2* gene ((NM\_014874): c.702G>A (p.Met234Ile)) described as probably pathogenic, the other inherited from the father on the *PMP22* gene ((NM\_000304): c.106A>G (p.Thr36Ala)) described as a variant of uncertain significance (VUS). The concomitant presence of the two mutations seems to have facilitated the appearance of the clinical phenotype, a severe form of axonal CMT caused by mitochondrial dysfunction.

We used an *in vitro* model of the disease using fibroblasts to study in detail the mitochondrial dynamic

## Materials and Methods

### Patients

The proband is a 16-year-old female patient who presented to our department with slowly progressive gait disorders since childhood. The first symptoms reported were difficulties with running and sporting activity and recurrent episodes of ankle twisting. At the age of 12, she noticed a real deficit of the foot lift muscles with steppage and more recently, the onset of quadridistal paresthesias and weakness of the upper limbs with difficulties in hand dexterity movements.

Clinical examination confirms a significant deformity with cavus varus foot and bilateral achilles retraction. She has generalized hyperreflexia. There is amyotrophy in all four limbs, predominantly in distal muscles and in low limbs, bilateral steppage on walking and attitudinal tremor of the upper limbs. Romberg's sign is positive.

The electrodiagnostic evaluation (EDX) shows a predominantly motor, axonal, length-dependent neuropathy. The motor conduction velocity of the median nerves is between 56 and 60 m/sec. The overall clinical-electrical picture is compatible with axonal Charcot-Marie-Tooth disease (CMT 2) (Table 1). Cerebral MRI and ocular evaluation were normal. The mother of the proband, originally from Italy, showed on clinical examination atrophy of the distal muscles of the lower limbs. The father, of Vietnamese origin, had a normal clinical examination. For both, the ENMG was normal except for the presence, on detection, of chronic neurogenic tracings on the two tibialis anterior muscles in the mother.

The pedigree is shown in Figure 1. The clinical and EDX data are shown in Table 1.

### Genetic analyses

The proband and her parents gave written informed consent in accordance with French law prior to blood sampling and skin biopsy. NGS was performed using an in-house designed panel containing the coding exons and flanking intronic sequences of neuropathy disease-associated genes. Then, we interpreted variant with the help of database as Online Mendelian Inheritance in ClinVar (<https://www.ncbi.nlm.nih.gov/clinvar/>), gnomAD (<https://gnomad.broadinstitute.org/>) and HGMD (<http://www.hgmd.cf.ac.uk>). Finally, following the American College of Medical Genetics and Genomics (ACMG) recommendations (Richards' classification, 2015), we classified the variants into five categories: pathogenic, likely pathogenic, variant of unknown significance (VUS), likely benign, and benign. Variants identified were confirmed by Sanger sequencing. Primer sequences and conditions for PCR and sequencing are available from the authors on request. The sequences were analyzed using Sequencher software.

**Table 1:** Clinical and neurophysiological data.

	P0	PI	PII
<b>Age</b>	16	62	53
<b>Age of onset (years)</b>	6	N	N
<b>Distal Weakness</b>			
<i>Upper limbs</i>	+++	N	N
<i>Lower limbs</i>	+	N	N
<b>Proximal Weakness</b>			
<i>Upper limbs</i>	N	N	N
<i>Lower limbs</i>	+	N	N
<b>Distal Atrophy</b>			
<i>Upper limbs</i>	+	N	N
<i>Lower limbs</i>	+++	N	+
<b>Proximal Atrophy</b>			
<i>Upper limbs</i>	N	N	N
Lower limbs	+	N	N
<b>Sensitivity</b>			
<i>Upper limbs</i>	N	N	N
Lower limbs	N	N	N
<b>Deep reflexes</b>	+++	N	+
<b>Pes cavus</b>	++	N	+
<b>MOTOR NERVES :</b>			
<b>Right Median Nerve</b>			
Distal latency (ms)	2.8	3.9	3.1
Distal cMAP (mV)	8.7	9	7.6
MCV (m/s)	60	56.4	53.8
<b>Right Peroneal Nerve</b>			
Distal latency (ms)	7	3.6	4.1
Distal cMAP (mV)	0.7	4.4	3.9
MCV (m/s)	36	51.9	47
<b>SENSORY NERVES</b>			
<b>Right Median Nerve</b>			
Distal SNAP (µV)	42	28.2	42
SCV (m/s)	63	54	57.8
<b>Right Sural Nerve</b>			
Distal SNAP(µV)	8.5	17.4	19.8
SCV (m/s)	36	56.6	51.4

## Cell Culture

After informed consent, skin samples were taken from the patient and from her parents. Primary cultures of fibroblasts were established using standard cell culture procedures. Briefly, the skin biopsy sample was cut into to small pieces then deposited directly on the surface of 60-mm culture dish in 600 µL culture medium (RPMI-1640 medium supplemented with 20% fetal calf serum, 50 µM 2-mercaptoethanol, 100 µM asparagine, 2 mM glutamine, and 1% penicillin/

streptomycin) in a humidified atmosphere with 5% CO<sub>2</sub> at 37 °C. After 3 days, as all skin samples are well attached to the bottom of the dish, 4 mL complete medium was added and allowed the culture to proceed. After 3-4 days of culture, the cells start to proliferate. When confluent, cells are transferred to a 100-mm culture dish for expansion. Medium was changed every other day.

A skin sample was also taken from an unrelated, unaffected individual (with no mutation in *MFN2* or *PMP22*). Cultured fibroblasts from the healthy individual were used throughout this work as a control sample.

## Immunofluorescence

Fibroblasts were passaged in a 48-well plate containing a coverslip. Cells were grown on the coverslip until the confluency reached 50 %. Cells were then fixed with 4% paraformaldehyde, and washed twice with PBS solution. They were next permeabilized with a PBS solution containing 0.2% tween 20, then exposed to a rabbit monoclonal antibody against PMP2 protein (Life Technologies SAS). After washing with PBS, cells were treated with a goat anti-rabbit secondary antibody coupled to the Alexa Fluor 488. Prior to mounting the coverslip on a slide, nuclei were labelled with DAPI. Images were taken using ZEISS LSM 880 confocal microscope.

## Electron microscopy

Cells were fixed in 1.6% glutaraldehyde in 0.1 M phosphate buffer (pH7.4). They were rinsed with cacodylate buffer 0.1 M, then post-fixed in osmium tetroxide (1% in cacodylate buffer) reduced with potassium ferricyanide (1%) during 1 h. Cells were washed once in water then dehydrated with several incubations in increasing concentrations of ethanol (from 30% to 100%) and embedded in epoxy resin (EPON). Eighty nanometer sections were contrasted with uranyl acetate (4% in water) then lead citrate and observed with a Transmission Electron Microscope (JEOL JEM 1400) operating at 100 kV and equipped with an Olympus SIS MORADA camera.

## Mitochondrial membrane potential

To establish the mitochondrial membrane potential in live fibroblasts, tetramethylrhodamine ethyl ester (TMRE) was used. TMRE is a cell permeant fluorescent dye that accumulates inside the cells according to their state: depolarized mitochondrial membrane reduces the sequestration of the TMRE inside the cells. Cells (150 000), cultured in a 24-well plate, were incubated for 20 min at 37 °C with 200 nM TMRE, then washed with the regular culture medium, treated with 1% trypsin, and centrifuged at 2000 rpm for 10 min, resuspended in 200 µL PBS/FCS/EDTA medium, and analyzed with flow cytometry (using 488 nm

laser for excitation and at emission 575 nm), with the FACS Canto II (BD Biosciences) and FACS Diva software (BD Biosciences). Each value represents the average of the wells per cell type.

### Quantification of intracellular ATP content

ATP Measurements were performed using luminescent approach according to the manufacturer's instructions (ATPlite assay kit, Perkin Elmer). Briefly, fibroblasts were plated in a 24-well plate until reaching confluency. The day of experiment, culture medium was removed, cells were scraped and resuspended in a lysis buffer (100 µL, included in the kit) to allow measurement of intracellular ATP content.

Proteins contents were simultaneous quantified in each well using DC protein assay kit (Bio-Rad, USA), according to the manufacturer's instructions for data normalization: Values of ATP content are expressed in µmol of ATP per mg of proteins.

### Mitochondrial network sizing

For mitochondrial staining, cells were incubated in a 100 nM solution of MitoTracker red (Invitrogen) for 15 min. Medium was replaced by fibroblasts culture medium, incubated 2 h at 37°C and washed in PBS. The samples were fixed with 4% paraformaldehyde (Electron Microscopy Sciences), washed with PBS and mounted on glass slides using ProLong Gold Antifade reagent (Molecular Probes). The images were acquired on a ZEISS LSM 880 confocal microscope and deconvolved with Huygens Essential Software™ (Scientific Volume Imaging) using a theoretically calculated point spread function (PSF) for each of the dyes. All selected images were iteratively deconvolved with maximum iterations scored 40 and a quality threshold at 0.05. The deconvolved images were used for quantitative mitochondrial network analysis with Huygens Essentiel Software™ with the following standardized set of parameters: threshold = 15%, seed = 10% and garbage = 10. The quantitative data were further analyzed in Microsoft Excel and GraphPad Prism 9 (GraphPad Software). Mitochondrial network length was quantified for 45 to 52 randomly-selected individual cells. Data are represented as mean ± S.E.M. Differences were considered as significant if p<0.05.

## Results

### Patients and genotypes:

Next generation sequencing was performed on the proband. We identified one variant probably pathogenic in the *MFN2* gene (NM\_014874): c.702G>A (p.Met234Ile), inherited from her mother and a variant of uncertain significance (VUS) in the *PMP22* gene (NM\_000304): c.106A>G (p.Thr36Ala) inherited from her father (Figure 1).

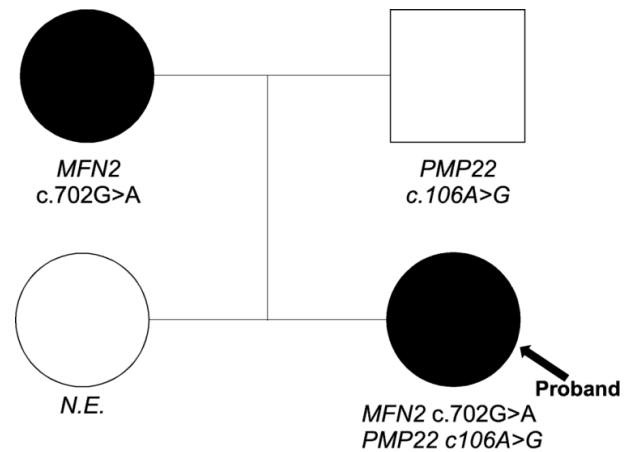


Figure 1: Pedigree and genotypes.

Symbols: squares for male, circles for females. Arrow: proband. Clinical status: n.e. = not examined; Genotypes: mutations indicated *MFN2* and *PMP22* are heterozygous

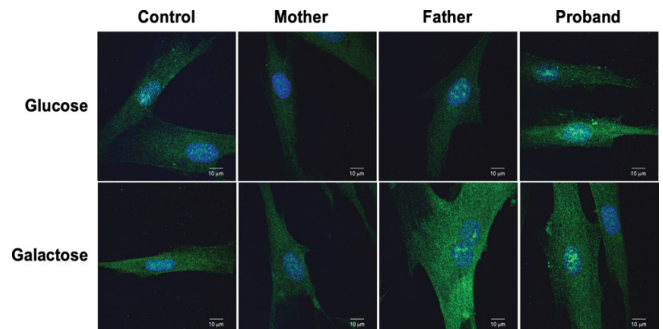


Figure 2: *PMP22* expression profile is not affected in fibroblasts  
Images of fibroblasts, from all family members, that were cultured in normal proliferation medium containing either glucose (25 mM) or galactose (10 mM). Images are representative of 3 independent cultures.

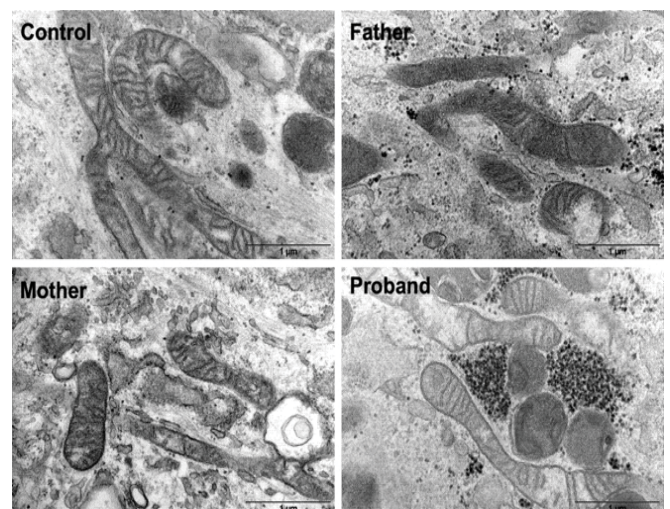


Figure 3: Fibroblasts have normal mitochondrial structure  
Electron microscopy images of fibroblasts of all family members and a control that were cultured in the presence of glucose (25 mM).

### PMP22 expression in fibroblasts

The localisation of PMP22 in fibroblasts was examined by immunofluorescence. No pathological PMP22 aggregates were found in the proband and control fibroblasts cultured either in presence of glucose (25 mM) or galactose (10 mM) (Figure 2).

### CMT fibroblasts have no phenotypical change

Mitochondria from normal and CMT cells, in glucose medium, visualized under electron microscopy showed no phenotypical difference (Figure 3). All genotypes showed normal phenotypical organization of the mitochondria structural compartments.

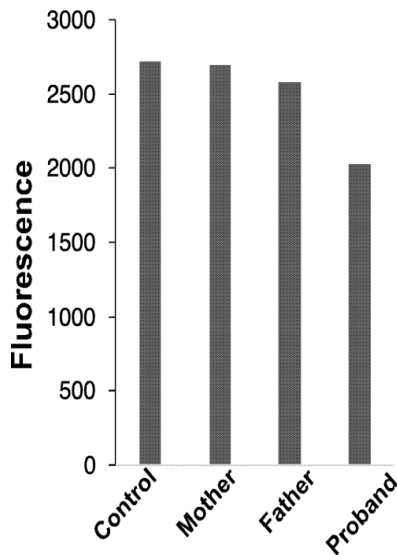


Figure 4: Mitochondrial membrane potential

Mitochondrial membrane potential was monitored in fibroblasts from all family members using TMRE as a membrane potential indicator

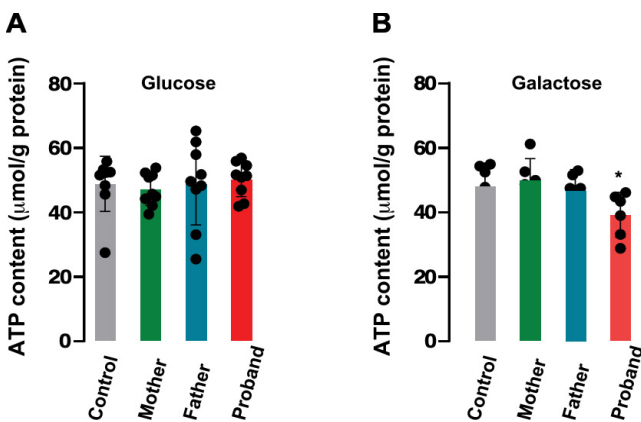


Figure 5: ATP content in patients' fibroblasts

ATP content was measured in all patients' fibroblasts either in the presence of 25 mM glucose (A) or 10 mM galactose (B). Values represent the mean ± SEM of three wells.

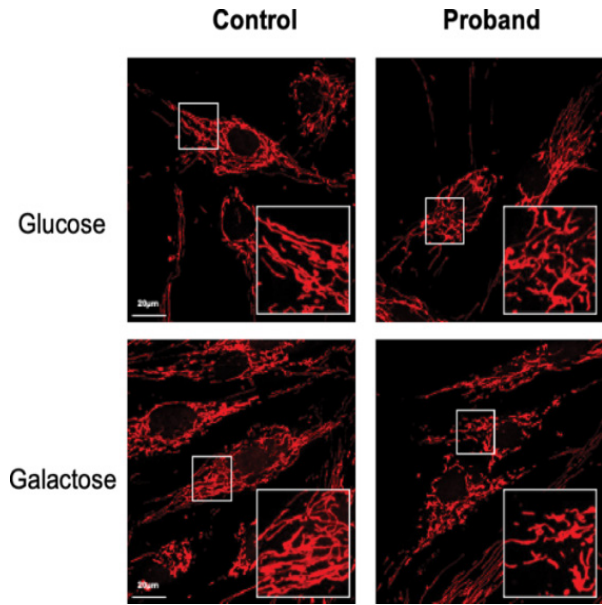


Figure 6: Mitochondrial network

Confocal images of mitochondrial network stained with MitoTracker Red for the control and the daughter fibroblasts, in glucose (25 mM) or galactose (10 mM) conditions. Culture in galactose medium allowed to observe a fragmentation of the mitochondrial network and less connected mitochondria in CMT patients compared to control fibroblasts.

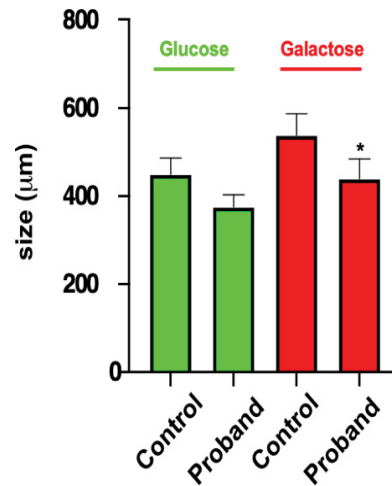


Figure 7: Mitochondrial network size

Size of the mitochondrial network was measured under glucose or galactose conditions for the control and the daughter fibroblasts. \*: using Anova test, only values between control and the proband cells were significantly different (p< 0.05).

### Mitochondria membrane potential ( $\Delta\Psi_m$ )

Since a mitochondrial dysfunction is often correlated with a change in mitochondrial oxidative phosphorylation, we measured the mitochondrial potential using the  $\Delta\Psi_m$ -sensitive fluorescent dye TMRE and FACS analysis. Interestingly, the

cells from the proband exhibits less fluorescence (reflecting a shift of  $\Delta\Psi_m$  towards of less-negative value, Figure 4) than cells from control or the patients carrying only one or the other mutation (mother, father).

### Intracellular ATP content.

ATP production was quantified in all genotypes in the presence of glucose or galactose. This strategy has been used to force the mitochondrial oxidative phosphorylation rather than glycolysis by substituting galactose for glucose in the growth media and to reveal mitochondrial dysfunction [24]. In the presence of glucose (Figure 5A) intracellular ATP content was not different in all cell type (n=6-9, independent experiments). However, when cultured in the presence of galactose, cells from the daughter showed a significant lower ATP content than the other cell types ( $39.20 \pm 2.84 \mu\text{mol/g}$  protein, proband;  $48.05 \pm 2.92 \mu\text{mol/g}$  protein, Control;  $p < 0.05$ ) (Figure 5B).

### Mitochondrial network sizing

Considering that MFN2 function is important for mitochondrial network organization, we compared the mitochondrial network of fibroblasts from CMT patient with that obtained from control fibroblasts. After staining with MitoTracker and examination by confocal microscopy, control fibroblasts displayed a typical filamentous interconnected network. In glucose medium, CMT patient fibroblasts presented with a mitochondrial network similar to control fibroblasts (Figures 5-6). Identical experiments were performed on fibroblasts grown in a glucose-free medium containing galactose. Culture in galactose medium allowed to observe a fragmentation of the mitochondrial network and less connected mitochondria in CMT patients compared to control fibroblasts. The length was in  $\mu\text{m}$ :  $536.8 \pm 48.5$  (n= 47) for control,  $438.4 \pm 44.5$  (n= 52) for the proband,  $408.69 \pm 26.3$  (n= 38) for the mother, and  $436.26 \pm 42.5$  (n= 29) for the father. Using Anova test, only values between control and the proband cells were significantly different ( $p < 0.05$ ) (Figures 6-7).

Confocal images of mitochondrial network stained with MitoTracker Red for the control and the daughter fibroblasts, in glucose (25 mM) or galactose (10 mM) conditions. Culture in galactose medium allowed to observe a fragmentation of the mitochondrial network and less connected mitochondria in CMT patients compared to control fibroblasts.

## Discussion

More than 100 pathogenic variants of the *MFN2* gene are known, mostly missense mutations that selectively target the GTPase domain and the coil-coiled region. We report for the first time the case of a patient with a heterozygous missense *MFN2* mutation (leading to the amino acid change Met234Ile) in the GTPase domain, which is likely to be associated with

CMT2A. Our study represents to our knowledge, the first analysis of changes in mitochondrial structure and function in a cell line of a patient carrying this genetic mutation.

From a clinical point of view, our patient presents a disabling neuropathy with an early onset, a progressive evolution and a motor impairment that predominates over sensory symptoms, which can be considered the classical phenotype of CMT2A, in its severe form. We did not find optic atrophy or brain lesions on MRI, but we did find pyramidal involvement and postural hands tremor. EDX shows preserved MCV, with variable reduction in the amplitude of compound muscle action potentials and distal sensory potentials, mainly in the lower limbs.

The mechanism underlying the pathogenesis of CMT2A has not yet been fully elucidated. Mitochondria play a key role in ensuring the efficient energy metabolism necessary for the proper functioning of peripheral nerves. The continuous process of fusion and fission, underlying mitochondrial dynamics, is crucial for the maintenance of the shape, size and number of mitochondria, as well as their axonal transport and their interaction with other organelles. Our CMT2A fibroblasts show no alterations in morphology but we found a decrease in mitochondrial bioenergetics. Similar findings have already been reported previously [25]. The absence of morphological changes could also be explained by the fact that fibroblasts express MFN1 which could compensate for some of the MFN2 deficit. In order to further stress the cell and reveal mitochondrial dysfunction, we replaced glucose with galactose in the growth medium, forcing fibroblasts to rely on mitochondrial oxidative phosphorylation [26]. Culture in galactose medium revealed a fragmentation of the mitochondrial network and less connected mitochondria in CMT patient compared to control fibroblasts corroborating the hypothesis of the pathogenic role of this mutation. This testifies to the fragility of the mitochondria, that are unable of meeting the cellular energy needs in aerobiosis as has already been described in senescent cells [27]. It can be speculated that cells with high ATP production requirements may be particularly vulnerable at the MFN2 deficit [28]. It is unclear whether the described mutation on the MFN2 gene causes an alteration of mitochondrial fusion resulting in ATP deficiency or whether it has a direct effect on bioenergetics [29] resulting in mitochondrial fragmentation. The reduction in membrane potential found appears to be secondary to dysfunctional mitochondrial coupling [30]. The scientific literature confirms that mitochondria with hyperpolarized membrane potential stagnating in the neuronal soma without ever reaching more crucial regions such as the growth cone or dendritic endings, as they are dysfunctional [31]. They will be later eliminated by autophagy [29].

What is surprising is that the above-mentioned changes

are found exclusively in the proband and not in the mother carrying the same genetic mutation. Genetic analysis did not reveal any substantial differences between the mother's genome and that of the proband except that the proband is the carrier of an additional mutation, the same VUS as the father in the *PMP22* gene. Myelin, like all glial cells, has been shown to supply lactate and glucose as an energy substrate for mitochondria to ensure axonal integrity [32]. We could speculate that the VUS found on *PMP22* gene may generate only partially functional *PMP22* protein. As *PMP22* is involved in maintaining myelin structure, this could alter communication with other internodal proteins and thus reduce the supply of energy substrate for the mitochondria. We can therefore speculate that we are facing a double trouble and that the presence of VUS on *PMP22* may promote the mitochondria dysfunction caused by the *MFN2* mutation. Mutations in *CASPR* or in *NF155* have already been shown to be responsible for the accumulation of mitochondria with abnormal morphology near the nodes [33],[34]. The pathogenetic hypothesis is therefore that impairment of myelin composition may facilitate alterations in the transport of already dysfunctional mitochondria. The absence of aggregation of *PMP22* in fibroblasts is probably due to the fact that VUS does not cause an excess of the protein like duplication but, rather, changes the configuration of the protein making it less functional. This hypothesis should be corroborated using other *in vivo* models.

## Conclusion

In conclusion, our data support the pathogenetic role of the c.702G>A *MFN2* mutation and indicate that a more complex gene regulatory mechanism is involved in determining the severity of the clinical phenotype. Analysis of mitochondrial function from fibroblast cultures proves to be a useful biomarker in the era of next-generation sequencing.

## Acknowledgments

Authors would like to thank the patients for their participation in this study. The study was supported by an Association Française contre les Myopathies (AFM) grant (#23207 to S.B.) and Agence Nationale pour la Recherche (ANR) grant (Labex ICST). We thank Sophie Pagnotta from CCMA (electron microscopy platform) for performing electron microscopy experiments.

## Statements and Declarations

The authors declare that no funds, grants, or other support were received during the preparation of this manuscript.

## Competing Interests

The authors have no relevant financial or non-financial interests to disclose.

## References

1. Barreto LCLS, Oliveira FS, Nunes PS et al. Epidemiologic Study of Charcot-Marie-Tooth Disease: A Systematic Review. *Neuroepidemiology* 46 (2016): 157–165.
2. El-Abassi R, England JD, Carter GT. Charcot-Marie-Tooth disease: an overview of genotypes, phenotypes, and clinical management strategies. *PM R* 6 (2014): 342–355.
3. Saporta ASD, Sottile SL, Miller LJ, et al. Charcot-Marie-Tooth disease subtypes and genetic testing strategies. *Ann Neurol* 69 (2011): 22–33.
4. Reilly MM. Sorting out the inherited neuropathies. *Pract Neurol* 7 (2007): 93–105.
5. Morena J, Gupta A, Hoyle JC. Charcot-Marie-Tooth: From Molecules to Therapy. *Int J Mol Sci* 20 (2019): E3419.
6. Li J, Parker B, Martyn C, et al. The *PMP22* gene and its related diseases. *Mol Neurobiol* 47 (2013): 673–698.
7. Feely SME, Laura M, Siskind CE et al. *MFN2* mutations cause severe phenotypes in most patients with CMT2A. *Neurology* 76 (2011): 1690–1696.
8. Züchner S. *MFN2* Hereditary Motor and Sensory Neuropathy. In: Adam MP, Everman DB, Mirzaa GM, et al., editors. *GeneReviews®*. Seattle (WA): University of Washington, Seattle, (1993).
9. Pipis M, Feely SME, Polke JM, et al. Natural history of Charcot-Marie-Tooth disease type 2A: a large (2013;) international multicentre study. *Brain* 143 (2020): 3589–3602.
10. Chung KW, Kim SB, Park KD, et al. Early onset severe and late-onset mild Charcot-Marie-Tooth disease with mitofusin 2 (*MFN2*) mutations. *Brain* 129 (2006): 2103–2118.
11. Choi B-O, Nakhro K, Park HJ et al. A cohort study of *MFN2* mutations and phenotypic spectrums in Charcot-Marie-Tooth disease 2A patients. *Clin Genet* 87 (2015): 594–598.
12. Lee M, Park C-H, Chung H-K et al. Cerebral white matter abnormalities in patients with charcot-marie-tooth disease. *Ann Neurol* 81 (2017): 147–151.
13. Brockmann K, Dreha-Kulaczewski S, Dechent P, et al. Cerebral involvement in axonal Charcot-Marie-Tooth neuropathy caused by mitofusin2 mutations. *J Neurol* 255 (2008): 1049–1058.
14. Muglia M, Zappia M, Timmerman V, et al. Clinical and genetic study of a large Charcot-Marie-Tooth type 2A family from southern Italy. *Neurology* 56 (2001): 100–103.

15. Chung KW, Suh BC, Cho SY, et al. Early-onset Charcot-Marie-Tooth patients with mitofusin 2 mutations and brain involvement. *J Neurol Neurosurg Psychiatry* 81 (2010): 1203–1206.
16. Lawson VH, Graham BV, Flanigan KM. Clinical and electrophysiologic features of CMT2A with mutations in the mitofusin 2 gene. *Neurology* 65 (2005): 197–204.
17. Lin H-P, Ho KWD, Jerath NU. Late onset CMT2A in a Family with an MFN2 Variant: c.2222T>G (p.Leu741Trp). *J Neuromuscul Dis* 6 (2019): 259–261.
18. Cartoni R, Martinou J-C. Role of mitofusin 2 mutations in the physiopathology of Charcot-Marie-Tooth disease type 2A. *Exp Neurol* 218 (2009): 268–273.
19. Fenton AR, Jongens TA, Holzbaur ELF. Mitochondrial dynamics: Shaping and remodeling an organelle network. *Curr Opin Cell Biol* 68 (2021): 28–36.
20. Yapa NMB, Lisnyak V, Reljic B, et al. Mitochondrial dynamics in health and disease. *FEBS Lett* 595 (2021): 1184–1204.
21. Vital A, Latour P, Sole G, et al. A French family with Charcot-Marie-Tooth disease related to simultaneous heterozygous MFN2 and GDAP1 mutations. *Neuromuscul Disord* 22 (2012): 735–741.
22. Meggouh F, de Visser M, Arts WFM, et al. Early onset neuropathy in a compound form of Charcot-Marie-Tooth disease. *Ann Neurol* 57 (2005): 589–591.
23. Cassereau J, Casasnovas C, Gueguen N, et al. Simultaneous MFN2 and GDAP1 mutations cause major mitochondrial defects in a patient with CMT. *Neurology* 76 (2011): 1524–1526.
24. Aguer C, Gambarotta D, Mailloux RJ, et al. Galactose enhances oxidative metabolism and reveals mitochondrial dysfunction in human primary muscle cells. *PLoS One* 6 (2011): e28536.
25. Amriott EA, Lott P, Soto J, et al. Mitochondrial fusion and function in Charcot-Marie-Tooth type 2A patient fibroblasts with mitofusin 2 mutations. *Exp Neurol* 211 (2008): 115–127.
26. Beręsewicz M, Charzewski Ł, Krzyśko KA, et al. Molecular modelling of mitofusin 2 for a prediction for Charcot-Marie-Tooth 2A clinical severity. *Sci Rep* 8 (2018): 16900.
27. Hutter E, Renner K, Pfister G, et al. Senescence-associated changes in respiration and oxidative phosphorylation in primary human fibroblasts. *Biochem J* 380 (2004): 919–928.
28. Hyun D-H, Lee J. A New Insight into an Alternative Therapeutic Approach to Restore Redox Homeostasis and Functional Mitochondria in Neurodegenerative Diseases. *Antioxidants (Basel)* 11 (2021): 7.
29. Loiseau D, Chevrollier A, Verny C, et al. Mitochondrial coupling defect in Charcot-Marie-Tooth type 2A disease. *Ann Neurol* 61 (2007): 315–323.
30. Twig G, Elorza A, Molina AJA, et al. Fission and selective fusion govern mitochondrial segregation and elimination by autophagy. *EMBO J* 27 (2008): 433–446.
31. Baloh RH, Schmidt RE, Pestronk A, et al. Altered axonal mitochondrial transport in the pathogenesis of Charcot-Marie-Tooth disease from mitofusin 2 mutations. *J Neurosci* 27 (2007): 422–430.
32. Nave K-A. Myelination and the trophic support of long axons. *Nat Rev Neurosci* 11 (2010): 275–283.
33. Sun X, Takagishi Y, Okabe E, et al. A novel Caspr mutation causes the shambling mouse phenotype by disrupting axoglial interactions of myelinated nerves. *J Neuropathol Exp Neurol* 68 (2009): 1207–1218.
34. Pillai AM, Thaxton C, Pribisko AL, et al. Spatiotemporal ablation of myelinating glia-specific neurofascin (Nfasc NF155) in mice reveals gradual loss of paranodal axoglial junctions and concomitant disorganization of axonal domains. *J Neurosci Res* 87 (2009): 1773–1793.